Journal of Ovonic Research Vol. 13, No. 2, March – April 2017, p. 55 - 62

STABILIZATION OF RESISTIVE SWITCHING IN Pt/HfO_x/NiO_y/Ni STACK BY LOCALIZED NANO-FILAMENTARY NUCLEATION OF OXYGEN VACANCIES

I. TALIB, M. ISMAIL, S. ANWAR, M. NAVID, M. Y. NADEEM*
Thin Films Lab, Department of Physics, Bahauddin Zakariya University, Multan-60800. Pakistan

The lack of spatio-geometrical control of conductive filaments in resistive switching oxides leads to operational dispersion and performance instability. We have experimentally demonstrated a method to localize the nucleation of conductive channels in Pt/HfO_x/NiO_y/Ni configuration via a sequential in situ cum ex situ electroforming process comprised of field-induced formation and local dissolution of intricately structured conductive percolation channels partially composed of oxygen-deficit and partially of metal-rich filamentary paths present respectively in the hafnia and NiO_y layers. The stable low power operation with fairly acceptable OFF/ON resistance ratio with only 8% loss in resistance window and feeble variation in operational parameters makes the demonstrated method a potential route for improving the performance of the future non-volatile memory devices. The improved operational stability has been found to be originated from the localization of the filamentary nucleation of oxygen vacancies in HfO_x layer just above the pre-formed single metallic filament in NiO_y layer.

(Received December 28, 2016; Accepted March 1, 2017)

Keywords: RRAM, electroforming, non-volatile memory, dual resistive switching, Electroforming, Oxygen vacancies

1. Introduction

The continuity of success in functional scaling of the conventional charge-storage based CMOS digital memory technology is going to reach its definitive limits till the end of this decade or so [1-2]. The realization of Moore's Law [3] have motivated an interest in the research community to identify promising, viable and unparalleled non-volatile memory approaches as a superior substitute to the conventional NVMs.

Resistive random access memory (RRAM) is an emerging next generation non-volatile information storage technology [4]. Due to their high degree of integrability [5], low-power operation [6,7], fast switching speed [8], resistive switching memories have attracted great attention as a future replacement of the existing flash memory. HfO_2, owing to its high melting point [9], large bulk modulus [10], high dielectric constant (22-25 [11], large band gap (5.8 eV [12], large refractive index [13], chemical stability and compatibility with the already existing CMOS technology [14], is being considered as one of the few most potential candidates for ReRAM applications**.**

In RRAM devices, the formation and reversible rupture of conductive filamentary channels is believed to play a key role in resistive switching phenomenon [15]. These conductive channels are formed spatially at random. This causes dispersion in operation and instability in performance. In the present work, we have experimentally demonstrated a comparatively an convenient method to affix the nucleation points of conductive filaments by using a dual oxide layer. We have first created stable Ni filaments in NiO_y layer in the first step of "in situ" electroforming, and then have used these metallic filaments as the preferred nucleation sites for the formation of oxygen-vacancy based nano-filamentary channels in the HfO_x matrix. This methodology not only stabilizes the operational voltages of the device but also enables it to exhibit

*Corresponding author: mynadeem.bzu@gmail.com

dual resistive switching behavior under the condition that the metallic filaments are not allowed to grow too strong during electroforming and the subsequent switching cycling.

2. Experimental

The n-type (100) Si substrate was washed for 15 minutes with deionized water (with 5% HF to remove native silicon oxide). Then 80 nm thick Ni layer was e-beam evaporated as the bottom electrode on to the pre-cleaned Si substrate. An NiO_y layer of nearly 20 nm thickness was grown by thermal oxidation in oxygen ambient (35% O_2 and 65% argon) in 35 minutes at substrate temperature of 380 ^oC. Now gold electrode dots of 60 nm thickness were deposited through a mask by e-beam evaporation. The pristine Au/NiO_y/Ni metal-insulator-metal stack was then subjected to negative electroforming process that occurred at -5.8 V with a compliance current set at 10 mA. After the sample was electroformed, the top Au electrode was chemically etched by potassium iodide solution (KI, I_2 and DI water in weight ratio 4:1:30) and then the sample was rinsed in DI water for 10 seconds, dried with nitrogen shower and finally backed at 60 ^oC in rough vacuum for 15 minutes to evaporate any residual etching liquid. Subsequently, HfO_x films with 18-22 nm thickness were deposited by reactive radio-frequency (RF) magnetron sputtering of pure hafnium target in oxygen cum argon ambient (with constant oxygen to argon ratio of 1:25) in about 40 minutes onto the NiO_y/Ni/Si stack preheated externally to 170-210^oC. Prior to the sputtering step, the vacuum chamber was evacuated to a base pressure of 2.5×10^{-4} Pa. The target-to-substrate distance was kept fixed at nearly 8 cm for all samples. Finally, the top Pt electrode was sputter patterned on to the HfO_x layer through a mask (with laser-cut circular holes. The schematics of the intermediate and the final forms of the device are shown in fig. 1(a & b).

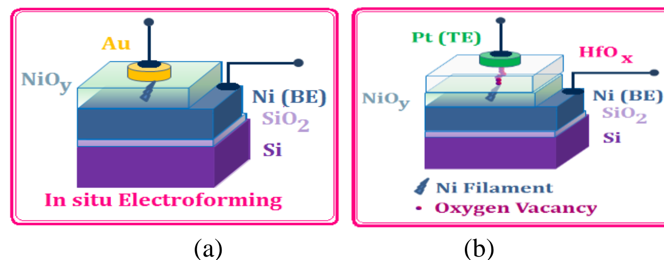

(a) (b)

Fig. 1 Schematic construction of
(a) intermediate Au/NiOy/Ni stack,
(b) final Pt/HfO_x/NiO_y/Ni stack

The degree of crystallinity in the auxiliary NiO_y and the active HfO_x layer was determined by glancing angle x-ray diffractometric (GAXRD) measurement by using Cuk_α radiation, while their chemical structure was determined by x-ray photoelectron spectroscopy by using standard monochromated Al Kα x-ray source (Hf=1486.6 eV) at normal takeoff (Thermo K-Alpha). To reduce the uncertainty, atomic percentages both in NiO_y and HfO_x were determined twice each and then averaged. The electrical characterization of the samples was performed by semiconductor parameter analyzer (Agilent 4156C). The electrical connection to the bottom Ni electrode was made by silver paste from the top after etching the oxide layers.

3. Results and discussion

Fig. 1(c) shows the x-ray diffractometric characterization of HfO_x films which were deposited by reactive magnetron sputtering on NiO_y/Ni/Si stacks kept at 210 ^oC. For the substrate temperatures 50-140 ^oC, the films were amorphous with no indication of any sort of macroscopic ordering.

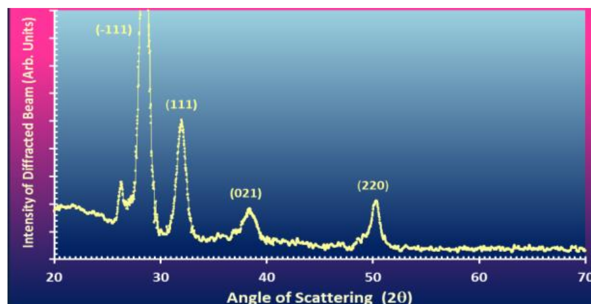

Fig. 1(c): XRD pattern of a representative HfO_x film deposited on NiO_y/Ni/ stack pre-heated to 210 ^oC

The observed dependence of the degree of crystallinity upon the substrate temperature indicates that the grain growth in HfO_x films is a thermally activated phenomenon. Deposition at substrate temperatures 170-210 ^oC produced polycrystalline films with nanometer sized crystallites (3.4-4.1 nm, as approximated by Debye-Scherrer relation). The x-ray diffraction pattern represented in Fig. 1 shows that the deposited HfO_x poly-crystallizes into monoclinic phase. The low intensity and large breadth of peaks riding over a bump on lower values of 2θ suggest that the oxide possesses nano-grains embedded in the amorphous matrix. In fact, poly crystalline HfO_x films can also be obtained by depositing amorphous HfO_2 films at room temperature and then inducing polycrystalline order via rapid thermal annealing (RTA, at >500 ^oC). But RTA is known to deteriorate the thermal and electrical stability of the material [16, 17].

Stoichiometric distribution of the constituents of the deposited nickel oxide and hafnia films were probed by high resolution core level x-ray photoelectron spectroscopy. The XPS analysis of the NiO_y layer, before it was electroformed, indicated that it is composed of stoichiometric oxygen content accompanied. This observation in combination with the XRD result (of NiO_y layer) suggest that the electroforming process might involve the formation of metallic filaments. Fig. 2(a) represents the primary peaks (which are characteristic of inner core Hf4f levels) of Hf.

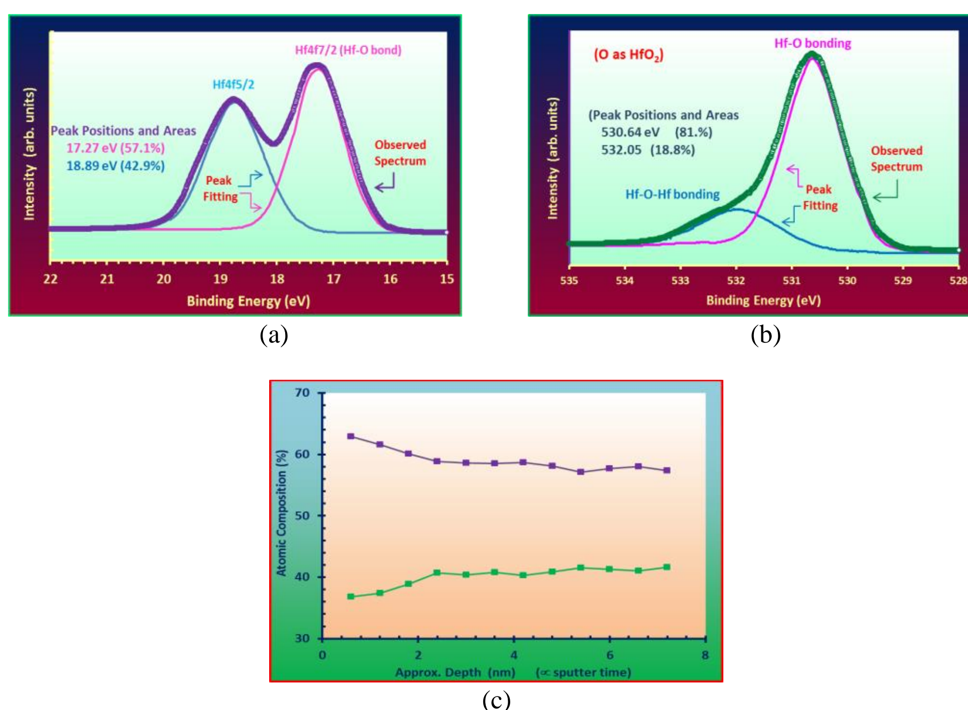

Fig. 2. (a) Core level Hf4f XPS spectrum, (b) Core level O1s XPS spectrum, (c) XPS based sputter depth profile of atomic composition

The primary region for the elemental XPS analysis of Hf is chosen to be the Hf4f region because this region of the XPS spectrum has distinct (well separated, Δ~1.68 eV) and intense spin-orbit components [18]. It is noteworthy that no peaks were observed at 14.2, 15.0 and 15.9 eV indicating that metallic Hf (i-e., un-oxidized Hf) is not present in the deposited HfO_x. The binding energy of Hf4f7/2 electron of a hafnium atom in Hf metal (where its oxidation state is 0) is 14.2eV, and that in stoichiometric HfO2 is 17.0 eV [19]. In Hf4f region, an asymmetrically shaped peak would correspond to Hf metal (Hf without any bonding with some other element), while a symmetric peak indicates the presence of some Hf compound such as an oxide. The intensity peak of Hf 4f7/2 observed at 17.27eVindicates the formation of Hf-O bonds and hence an evidence of the formation of HfO_x as well. This feature peak is separated by 1.62 eV from Hf 4f5/2 peak at 18.89 eV. In a stoichiometric HfO_2 sample (HfO_x with x=2), these peaks are observed at 16.8 eV and 18.5. As Hf has only a single oxidation state (it forms only a single oxide, namely HfO_2) so this chemical shift towards higher binding energy cannot be attributed to any valance change. Rather the observed shift in the feature peaks towards higher binding energy side is an indicative of the presence of Hf-rich, and hence oxygen deficit, HfO_x. In Fig. 2(b), O1s region is the primary XPS region for identification of the presence of oxygen in a given sample. In metal oxides, O1s peak lies within 529-531 eV range. Fig. 2(b) shows the O1s XPS spectrum in the form of an envelope that has been fitted by two de-convoluted Gaussian peaks. The smaller peak is due to organic contaminants (hydrocarbons) present as residual in the vacuum chamber. The shift of the location of the O1s peak from its normal position at 530.64eV to the higher energy side at around 532 eV indicates that the chemical state of Oxygen is affected due to O-defects in the sample. The observed chemical shift towards higher binding energy can be attributed to a decrease in the number of Hf-O bonds and a proportional increase in the number of stronger Hf-Hf bonds, thus leading to a non-stoichiometric character (HfO_x with $x<2$)accompanied by oxygen vacancies in the metal oxide matrix. The decrease in the Hf-O bonds and the associated increase in Hf-Hf bond can be understood by the distribution of oxygen atoms. As O atoms are bonded with Hf atoms (O-Hf-O) and not with O atoms (Hf-O-O), so an oxygen vacancy can definitely be expected to be created near a Hf atom rather near an oxygen atom, resulting in a decrease in Hf-O bonds and an increase in Hf-Hf bonds.

The sputter depth profile in the Fig. 2(c) shows that the deposited hafnia films are not stoichiometric. Rather the atomic ratio of Hf and oxygen is on the average 1:1.42, as determined by considering the relative areas of the Hf4f doublets and O1s peaks. This considerably reduced oxygen content is a clear indication of the presence of defects named as oxygen vacancies in the HfO_x layer.

The NiO_y layer in the Au/NiO_y/Ni stack was subjected to a ramped negative voltage sweep which electroformed the stack at -5.8 V. The IV-curve of electroforming process and the subsequent positive IV-sweep in the presence of current compliance are shown on semi-logarithmic scale in Fig. 3(a) and on linear scale in Fig. 3(b).

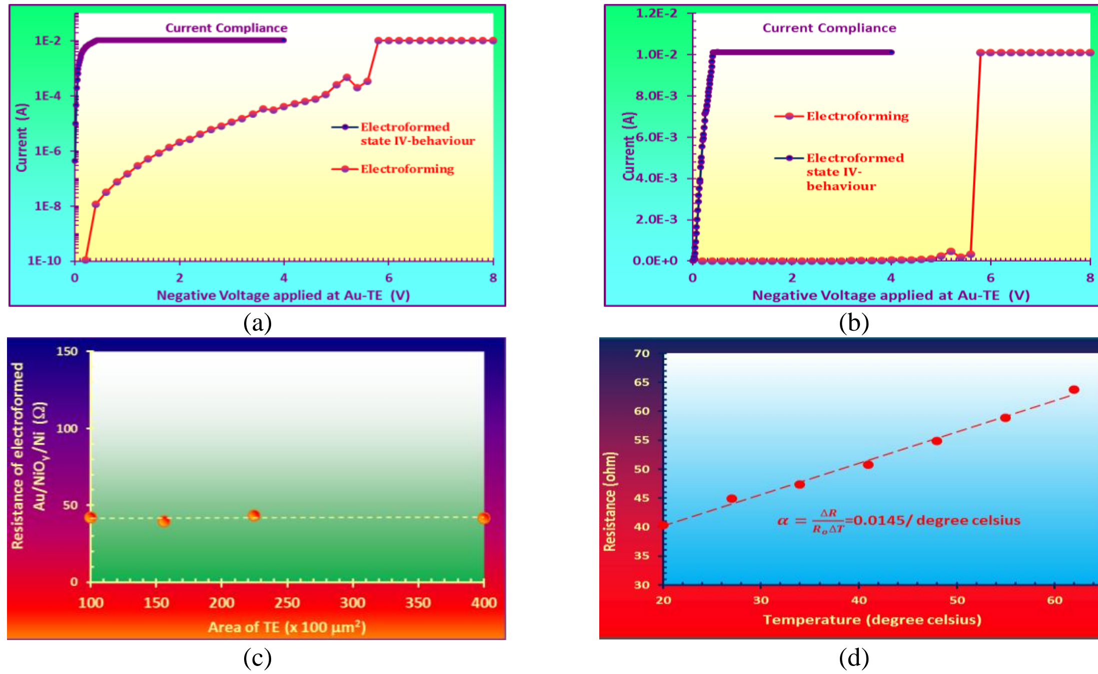

Fig. 3: Electroforming of Au/NiOy/Ni stack, and IV-behavior after electroforming on semi-logarithmic scale (a) and linear scale (b), (c) Dependence of resistance of the electroformed state of Au/NiOy/NI stacks on the area of the top electrode, (d) Variation of the resistance of the electroformed Au/NiOy/Ni stack with temperature.

It is quite evident from the Fig 3(a) and 3(b) that for a given applied voltage, the current through the electroformed Au/NiO_y/Ni stack is by an order of magnitude larger than that in the pre-electroformed stack. In order to elucidate the possible reason for an order of magnitude increase in the conductivity of the stack, the resistance of the electroformed Au/NiO_y/Ni stacks with different top electrode areas was measured as a function of the top electrode area for a fixed reading voltage of 0.15 V. Fig. 3(c) shows that the resistance of the electroformed state of Au/NiO_y/Ni stack is independent of the area of the top electrode. This lack of scaling of the resistance of the electroformed Au/NiO_y/Ni stack with the cell cross-section provides an experimental evidence for two conclusions. Firstly, the observed electroforming of the interposed NiO_y dielectric leads to localized filamentary-type conduction. Secondly, there is only a single filament that is predominantly formed within the NiO_y matrix during the electroforming process. This conclusion is quite reasonable because if there were many conductive filaments produced in parallel with one another through the electroformed NiO_y stack, the change in the area of the top electrode would have affected the magnitude of current through the electroformed stack. Our conclusion that switching is dominantly controlled by the formation and local rupture of a single filament of metallic islands is further supported by small decrease in the electroformed state resistance during first few repeated IV-sweeps.

Fig. 3(b) shows that the conduction in the electroformed NiO_y layer is of Ohmic nature. For further clarification, temperature dependence of the resistance of the electroformed state of NiOy was investigated. The metal-like behavior of the resistance of the electroformed Au/NiO_y/Ni stack over a considerable temperature range, as represented in Fig. 3(d), suggests that the single conductive filament formed within, and during the electroforming of, NiO_y layer is surely of metallic nature. On the contrary, if the conductive filament was composed of oxygen-vacancies, it would have shown semiconductor like temperature dependence of resistance. This formation of the metallic filament is compatible with the XPS measurements where the NiO_y layer was found to have greater oxygen content than in stoichiometric NiO_y (NiO_y with y=1). No doubt, O^{2-} ions may be expected to diffuse towards the anode creating behind oxygen vacancies but it is most likely that Ni ions diffuse to a greater extent towards the cathode than the oxygen ions towards the anode. This can actually be expected due to a number of reasons. In the first place, due to the

absence of abundant oxygen vacancies (as indicated by XPS results), self-diffusion of Ni ions can be expected to be greater than that of O-ions (and oxygen vacancies). Secondly, since the deposited NiO_y is polycrystalline, so the presence of grain boundaries is suspected to be helpful for Ni migration preferentially along the grain boundaries. Thirdly, Ni is experimentally known to be an electrochemically active material with relatively high diffusivity. Hence, NiO_y will behave like a solid electrolyte, and the ionic diffusion through it can be expected to be strongly governed by its degree of crystallinity. These factors cause the formation of a metallic filament during the electroforming process.

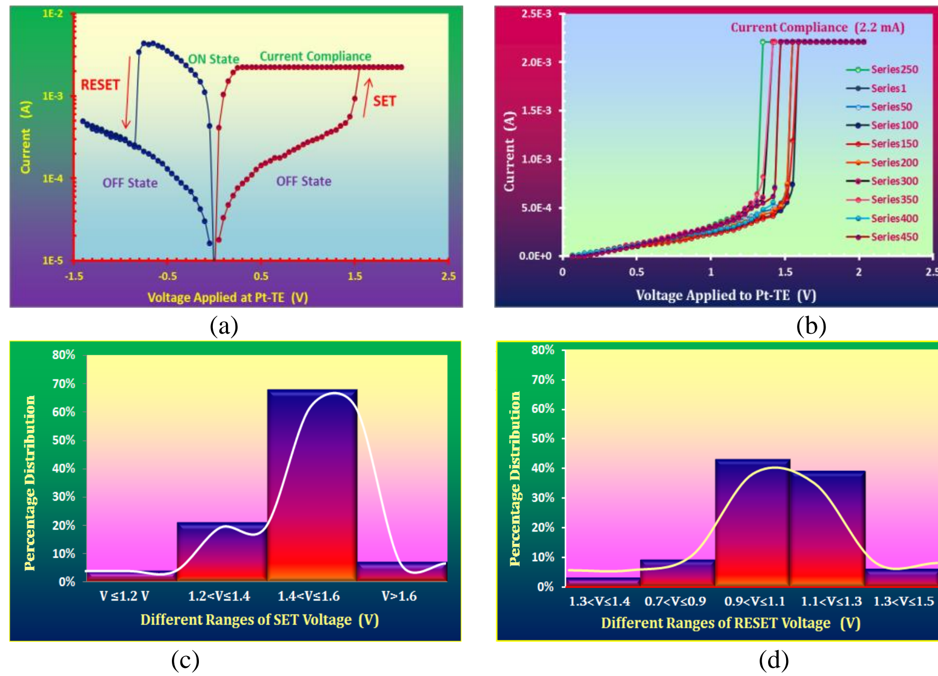

Fig. 4: (a) A representative bipolar resistive switching cycle of the Pt/HfO_x/NiO_y/Ni device comprised of set and reset operations, (b) SET parts of different resistive switching cycles (CC=2.2 mA), (c) Percentage distribution of SET voltages in resistive switching cycles, (d) Percentage distribution of RESET voltages in resistive switching cycles

Fig. 4(a) displays a representative bipolar resistive switching cycle of the final Pt/HfO_x/NiO_y/Ni device. The prominent increase in the current level under the applied voltage during the SET process is usually attributed to the formation of low resistance channel(s). We attribute the formation of these fine current paths, called as conductive filaments, to the field-induced piling up of oxygen vacancies along the grain boundaries in the polycrystalline HfO_x. The probability that the conductive path(s) are made up of Hf metal instead of OVs is very small because in an oxygen deficient oxide layer the diffusion of oxygen ions (and hence OVs) would be much easier than that of Hf metal cations. The abrupt increase in the current in the forming process of HfO_x indicated that owing to the pre-existing Ni-filament in NiO_y layer, it takes a little electrical energy to trigger the device into its ON state. Fig. 4(b) shows the setting parts of different resistive switching cycles subsequent to the forming process. The values of SET voltage can be noticed to be smaller than what have been reported in similar HfO_x based devices. Most importantly, there is very small dispersion in the SET voltage. Fig. 4(c) indicates that the distribution of Vset is limited to a narrow voltage range. We attribute this stabilization of the operating voltage to the localization effect of the oxygen-vacancy-based conductive filaments in the HfO_x layer by the Ni filaments present in the underlying NiO_y layer. The concentrated field at the tip of Ni-filaments right below the HfO_2 layer not only enhances the diffusion of oxygen vacancies under the applied field but also ensures that at one time only one filament is created. In the ON state of the device, current flows in NiO_y mainly through the Ni filament present in it, while in HfO_x layer it passes mainly through the OVs-based filament. So in ON state, the conductive filament can be viewed as

an intricately structured filament partly composed of metallic filament and partly of OVs-based filament. Subsequently, when a negative voltage is applied to the top electrode, the device switches back to high resistance state (negative reset). Definitely this can happen when one of the two parts of the intricately structured filament is dissolved. The MIM based ReRAM devices with metallic filaments are known to require higher set and reset voltages than the devices with OVs-based filaments. On the basis of this established fact, it can be justifiably assumed that the reset takes place due to local rupture of the OVs-based filament present in HfO_x. Fig. 4(d) displays the distribution of reset voltage with consecutive memory switching cycling. It shows that whereas the localization effect of filamentary nucleation of oxygen vacancies in HfO_x plays a profound role in reducing the dispersion in set voltage distribution, it has relatively smaller impact on the reset voltage distribution.

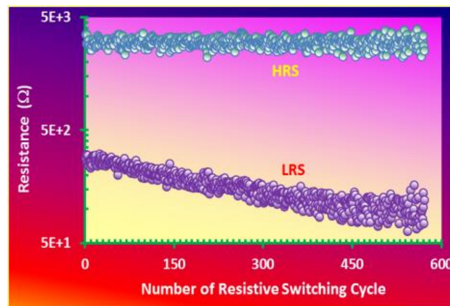

Fig. 5: Stability in LRS and HRS with repeated resistive switching cycles

Fig. 5 shows that during about 0.6×10^3 resistance switching cycles we have measured, the OFF state resistance remains almost stable, while the ON state resistance slightly decreases with repeated cycles. Whereas a further investigation is needed to explain this slight decrease in LRS, we here suggest that the possible reason for the decrease in the ON-state resistance with successive cycling might be due to a field induced diffusion of the Ni species from the Ni filament present in the lower oxide layer (NiO_y) into the upper oxide layer (HfO_x) during negative RESET process.

The different states of the device during its fabrication, electroforming and resistive switching are illustrated in Fig. 6 (a to f). It can be noticed that the Ni filament plays the dominant role in localizing the conductive filament composed of oxygen vacancies. This also adds an additional contribution to the observed reduced dispersion of the operating voltages. The observed stability in operation and performance in repetitive resistive switching cycling makes it evident that the demonstrated method is very promising for potential applications in ReRAM memory technology due to its ability to avoid any randomized nucleation of oxygen vacancies in the active memory oxide layer.

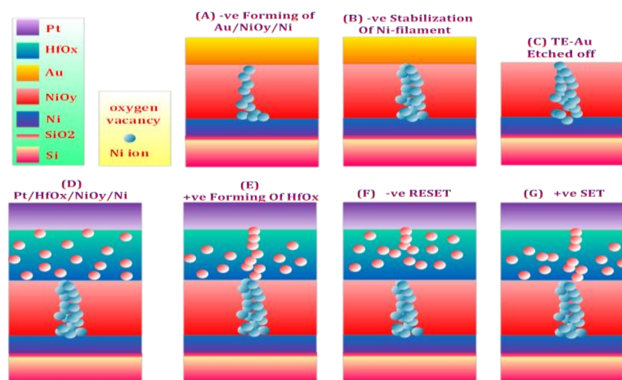

Fig. 6: Different states of the device, (a) $Au/NiO_y/Ni$ stack after negative forming and filament stabilizing step, (b) electroformed NiO_y layer after chemical removal of top Au electrode, (c) $Pt/HfO_x/NiO_y/Ni$ stack in pristine form, (d) the stack after forming step, (e) RESET, (f) SET

4. Conclusions

Via a two-step electroforming of a double layered oxide structure, the metallic filament(s) present in the lower oxide can provide the preferred starting point(s) for the oxygen vacancy based filamentary path(s) in the upper oxide layer. This not only reduces the operational voltages but also restricts their values (particularly, the set voltage) in a narrow range ultimately leading to a stabilized performance of the resistive switching device.

The device can be made to show only bipolar or dual resistive switching behavior merely by controlling the strength of the metallic filament formed in the lower oxide layer. The absence of resistance scaling of the electroformed lower oxide with the top electrode area may provide an additional degree of freedom for device scaling if the same property is possessed by the top upper oxide layer.

Acknowledgments

Authors acknowledge the financial support by Higher Education Commission (HEC), Islamabad Pakistan under the International Research Support Initiative Program (IRSIP).

References

[1] K. J. Kuhn, IEEE Transactions on Electron Devices, **59**, 1813 (2012).
[2] S. S. Binti Md Sallah, H. Mohamed, M. Mamun, Md. S. Amin, J. Appl. Sci. Res. **8**, 4138 (2012).
[3] C. A. Mack, IEEE Trans. Sem. Manu. **24**, 202 (2011).
[4] A. Sawa, Mat. Today **11**, 28 (2008).
[5] D.-H. Kwon, K. M. Kim, J. H. Jang, J. M.Jeon, M.H. Lee, G. H. Kim, X.-S Li, G.-Su Park, B. Lee, S. Han, M. Kim andC. S. Hwang, Nat. Nano. **5**, 148 (2010).
[6] H.-L.-Y. Lee, P.-S. Chen, C.-C Wang, S. Maikap, P.-J.Tzeng, C.-H Lin, L.-S. Lee, M.-J Tsai, Jap. J. App.Phy. **46**, 2175 (2007).
[7] S. Z. Rahaman, S.Maikap, T.-C, Tien, H-Y Lee, W-S Chen, F. Chen, M.J Kao, M-J Tsai, Nano. Res.Lett. **7,** 345 (2012).
[8] A. Prakasha, S. Maikapa, C.S. Laia, T.C. Tienb, W.S. Chenc, H.Y. Leec, F.T. Chenc, M.-J. Kaoc, M.-J. Tsaic, Sol.-St. Elec. **77**, 35 (2012).
[9] F. L. Martínez, M. T.-Luque, J. J.Gandía, J.Cárabe, W.Bohne, J.Röhrich, E.Strub, I.Mártil, J. Phys. D: App.Phy. **40**, 5256 (2007).
[10] R. Wu, B. Zhou1, Q. Li, Z. Jiang, W. Wang, W. Y. Ma and X. Zhan, J.Phy. D: App. Phy. 45, 0022-3727 (2012).
[11] C. T. Hsu, Y. K.Su and M., Japanese Yokoyama, Jpn. J. Appl. Phys. **31**, 2501(1992)
[12] J. Choi, R. Puthenkovilakam and J. P. Chang,J. Appl. Phys. **99**, 053705 (2006)
[13] W. J. Bae, M. Trikeriotis, J. Sha, E. L. Schwartz,R. Rodriguez, P. Zimmerman, E. P. Giannelisa and C. K. Ober, J. Mater. Chem. **20**, 5186 (2010).
[14] Y.-S. Lin, R. Puthenkovilakam and J. P. Chang, Appl. Phys. Lett. **81**, 2041 (2002)
[15] R. Waser and M. Aono, Nature Materials **6**, 833 (2007)
[16] B. K. You, W. I. Park, J. M. Kim, K. Park, H. K. Seo, J. Y. Lee, Y. S. Jung, K. J. Lee, ACS Nano **8**, 949 (2014).
[17] N. Zhan,M.C. Poon, C.W. Kok, K. L.Ng, H. Wong J. Electrochem. Soc. **150**(10), F200 (2003)
[18] C. W. Joon, L. E. Joung, Y.K. Soo, Y. J. Yup, L. J. Hyun, K. K.Chae, H. J.Pyo, K. I. Jae, J. Kor.Phy. Soc.**45**, 716 (2004)
[19] J. Koo and H.Jeon, J. Kor.Phy. Soc. **46**, 945 (2005).